Assessment of Wind Parameter Sensitivity on Ultimate and Fatigue Wind Turbine Loads

Preprint

Amy Robertson, Latha Sethuraman, Jason Jonkman, and Julian Quick
National Renewable Energy Laboratory

Presented at the American Institute of Aeronautics and Astronautics SciTech Forum
Orlando, Florida
January 8–12, 2018

Suggested Citation
Robertson, Amy, Latha Sethuraman, Jason Jonkman, and Julian Quick. 2018. "Assessment of Wind Parameter Sensitivity on Ultimate and Fatigue Wind Turbine Loads: Preprint." Golden, CO: National Renewable Energy Laboratory. NREL/CP-5000-70445. www.nrel.gov/docs/fy18osti/70445.

NREL is a national laboratory of the U.S. Department of Energy
Office of Energy Efficiency & Renewable Energy
Operated by the Alliance for Sustainable Energy, LLC

This report is available at no cost from the National Renewable Energy Laboratory (NREL) at www.nrel.gov/publications.

Conference Paper
NREL/CP-5000-70445
February 2018

Contract No. DE-AC36-08GO28308

NOTICE

This report is available at no cost from the National Renewable Energy Laboratory (NREL) at www.nrel.gov/publications.

Available electronically at SciTech Connect http:/www.osti.gov/scitech

Available for a processing fee to U.S. Department of Energy and its contractors, in paper, from:

U.S. Department of Energy
Office of Scientific and Technical Information
P.O. Box 62
Oak Ridge, TN 37831-0062
OSTI http://www.osti.gov
Phone: 865.576.8401
Fax: 865.576.5728
Email: reports@osti.gov

Available for sale to the public, in paper, from:

U.S. Department of Commerce
National Technical Information Service
5301 Shawnee Road
Alexandria, VA 22312
NTIS http://www.ntis.gov
Phone: 800.553.6847 or 703.605.6000
Fax: 703.605.6900
Email: orders@ntis.gov

Cover Photos by Dennis Schroeder: (left to right) NREL 26173, NREL 18302, NREL 19758, NREL 29642, NREL 19795.

NREL prints on paper that contains recycled content.

Assessment of Wind Parameter Sensitivity on Ultimate and Fatigue Wind Turbine Loads

Amy N. Robertson,[*] Latha Sethuraman,[†] Jason Jonkman,[‡] Julian Quick[§]
National Renewable Energy Laboratory, Golden, CO , 80401

Wind turbines are designed using a set of simulations to ascertain the structural loads that the turbine could encounter. While mean hub-height wind speed is considered to vary, other wind parameters—such as turbulence spectra, sheer, veer, spatial coherence, and component correlation—are fixed or conditional values that, in reality, could have different characteristics at different sites and have a significant effect on the resulting loads. This paper therefore seeks to assess the sensitivity of different wind parameters on the resulting ultimate and fatigue loads on the turbine during normal operational conditions. Eighteen different wind parameters are screened using an Elementary Effects approach with radial points. As expected, the results show a high sensitivity of the loads to the turbulence standard deviation in the primary wind direction, but the sensitivity to wind shear is often much greater. To a lesser extent, other wind parameters that drive loads include the coherence in the primary wind direction and veer.

I. Introduction

Wind turbines are designed using the International Electrotechnical Commission (IEC) 61400-1 standard,[1] which prescribes a set of simulations to ascertain the ultimate and fatigue loads that the turbine could encounter under a variety of environmental and operational conditions. In the simulation prescription, a range of mean hub-height wind speeds are considered, but other wind parameters—such as the turbulence spectra, sheer, veer, spatial coherence, and component correlation—are fixed values that remain constant across all simulations,[**] or are conditioned only on wind speed,[††] the IEC classification of turbulence, and/or hub height. These other wind parameters, however, could have different characteristics at different sites and under different atmospheric conditions, which could potentially have a significant effect on the resulting loads the turbine could see. Therefore, this paper seeks to assess the sensitivity of different wind parameters on the resulting loads of the wind turbine, to 1) rank the sensitivities of different parameters, 2) help establish error bars around the predictions of engineering models during validation efforts, and 3) provide insight to probabilistic design methods and site-suitability analyses.

Other researchers have examined the influence of wind characteristics on turbine load reponse, considering differing wind parameters and turbulence models, and using different methods to assess their sensitivity. The most common parameter considered is the influence of turbulence intensity variability, which all researchers show to have significant variability and large impact on the turbine response.[2-16] The shear exponent, or wind profile, is the next most common parameter examined, concluded to have similar or slightly less importance to the turbulence intensity.[3,5,6,9,10,13-15,17] Other parameters investigated include the turbulence length scale, standard deviation of different directional wind components, Richardson number, spatial coherence, component correlation, and veer. Mixed conclusions are drawn on the importance of these secondary parameters, which are influenced by the range of variability considered (based on the conditions examined), the turbine control system, as well as the turbine size and hub height under consideration. The effects of considering the secondary wind parameters are also mixed, sometimes increasing and sometimes decreasing the loads in the turbine; however, most agree that the use of site-specific measurements of the wind parameters will lead to a more accurate assessment of the turbine loads, resulting in designs that are either better optimized or lower risk.

Another approach used by many researchers is to examine how the stability of the atmosphere affects the loading conditions, which dictate the correlation between the individual atmospheric parameters for each stability condition

[*] Senior Engineer, National Renewable Energy Laboratory, 15013 Denver West Parkway, Golden, CO 80401
[†] Post Doctorate, National Renewable Energy Laboratory, 15013 Denver West Parkway, Golden, CO 80401
[‡] Senior Engineer, National Renewable Energy Laboratory, 15013 Denver West Parkway, Golden, CO 80401
[§] Research Associate, National Renewable Energy Laboratory, 15013 Denver West Parkway, Golden, CO 80401
[**] For example, the power-law shear exponent is taken to be 0.2 for the normal wind profile.
[††] For example, the turbulence standard deviation in the primary wind direction is taken to be the 90% quantile for the given hub-height wind speed based on an assumed log-normal distribution of turbulence.

and also different models of the turbulence and shear.[2,3,6,9,18,19] Holtslag et al.[2] conclude that the IEC standards have the potential to overestimate fatigue loads from unrealistic combinations of shear and turbulence, but also underestimate loads by neglecting the assessment of strongly unstable conditions. They propose a computationally efficient approach of simulating the most probable stability condition for each wind speed bin as an improvement over the present IEC methodology.

Our concern in this paper is to obtain a thorough assessment of which wind characteristics influence wind turbine structural loads. Our approach does not consider the correlated dependency between the individual parameters; rather, we focus on assessing the sensitivity of each parameter individually (but interactions between individual parameters are also considered, which is further discussed below). This is a first step in understanding what modifications might be needed to present design loads analysis or site-suitability methods and could inform how error bars are established on model predictions in future validation efforts. By understanding which wind parameters actually have an influence on response, we can then consider the best way to address the influence of their variation or uncertainty.

The remainder of the paper is organized as follows. Section II summarizes the different wind parameters considered in this study and prescribes a range over which they will be varied. Section III presents the methodology used to screen which of these parameters have a significant effect on key wind turbine response loads. Section IV then describes the steps used (and associated details) to conduct the simulations needed for the analysis. Finally, Sections V and VI present the results of the sensitivity analysis and the conclusions that were drawn.

II. Wind Parameter Description

The first step in this work is to determine the relevant wind parameters that will be used to represent the variety of inflow conditions that a turbine can encounter during operation. We have chosen to use the Veers model for describing and generating the wind characteristics because it provides a quantitative description with a known and limited set of parameters. Based on this model, 18 different wind parameters (Table 1) are used to parameterize the following wind characteristics: (A) mean wind profile, (B) velocity spectrum, (C) point-to-point spatial coherence, and (D) component-to-component correlations. For simplicity, we assume that these 18 parameters are independent of one another.

The parameters are only conditioned on mean wind speed at hub height, and their range (summarized in Section E) is specified based on a categorization in below-rated, near-rated, or above-rated wind regions. The sensitivity analysis will be run three separate times across these three separate wind regions, assuming a mean wind speed within each bin (8, 12, and 18 m/s). No specific site is considered; rather, the parameter ranges are chosen to span a large sampling of potential wind turbine locations. TurbSim[20] is used to generate the turbulent wind time series based on the parameters chosen.

A. Mean Wind Profile

A standard power-law shear model is used to describe the vertical wind speed profile and a linear wind direction veer model is used. The sensitivity of these characteristics are captured through variation of the exponent of the shear, α, and the total veer (in degrees) across the turbine, β (centered around the hub) (red highlight indicates the individual parameters that will be investigated).

B. Velocity Spectrum

The Veers model uses a Kaimal spectrum to represent the turbulence, which differs slightly from the other commonly used Mann turbulence model (see below). The Kaimal spectrum is defined as:[1]

$$\frac{fS_q(f)}{\sigma_q^2} = \frac{4fL_q / V_{hub}}{(1+6fL_q / V_{hub})^{5/3}}, \tag{1}$$

where f is the frequency (Hz), q is the index of the velocity component direction (u, v, w), S_q is the single-sided velocity spectrum, V_{hub} is the mean wind speed at hub height, σ_q is the velocity component standard deviation, and L_q is the velocity component integral scale parameter. The IEC 61400-1 standard[1] suggests using a set scaling between the direction components of the standard deviation and scale parameters, but for our study we will vary each of these parameters in (u, v, w) independently.

An inverse Fourier transform is applied to the Kaimal spectrum to derive a turbulent time series for each of the wind components independently. Note that this is different from the Mann model (also considered in the IEC 61400-1 standard), which is based on a three-dimensional tensor representation of the turbulence derived from rapid

distoration of isotropic turbulence using a uniform mean velocity shear.[21] The Mann model considers the three turbulence components as dependent, representing the correlation between the longitudinal and vertical components resulting from the Reynolds stresses. In the IEC 61400-1 standard, the two spectra (Mann and Kaimal) are equated, resulting in three parameters that may be set for the Mann model. However, there is uncertainty in whether the loads resulting from these two different turbulence spectra are truly consistent.

C. Spatial Coherence Model

The point-to-point spatial coherence (*Coh*) quantifies the frequency-dependent cross-correlation of a single turbulence component at different points in the wind inflow grid. The general coherence model used in TurbSim, which includes all three directions of the velocity components, $q = u, v, w$, is defined as:

$$Coh_{i,j_q,f} = \exp\left(-a_q \left(\frac{d}{z_m} \right)^{\gamma} \sqrt{\left(\frac{fd}{u_m} \right)^2 + \left(b_q d \right)^2} \right), \tag{2}$$

where f is the frequency, d is the distance between points i and j, z_m is the mean height of the two points, and u_m is the mean of the wind speeds of the two points.[‡‡] The variables a_q and b_q are, respectively, the input coherence decrement and offset parameter (for each velocity component, q). The model is based on the IEC coherence model with the added term, $(d/z_m)^{\gamma}$, introduced by Solari,[12] where γ can vary between 0 and 1.

D. Component Correlation Model

The component-to-component correlation (*PC*) quantifies the cross-correlation between directional turbulence components at a single point in space. For instance, PC_{uw} quantifies the correlation between the u and w turbulence components at a given point. TurbSim modifies the v- and w-component wind speeds by computing a linear combination of the time series of the three independent wind speed components to obtain the mean Reynolds stresses, PC_{uw}, PC_{uv}, PC_{vw}, at the hub. Note that because this calculation occurs in the time domain, the velocity spectra of the v- and w-components are somewhat affected by the enforced component correlations.

E. Parameter Ranges

The ranges considered for each of these 18 parameters within the three different wind speed bins are summarized in Table 1. For some parameters, no information was found on their dependence on wind speed, so the same values are used in all three bins. The ranges are taken from multiple sources[2-34] (those references driving the extremes of the range are cited below the values), largely based on measurements across a variety of different locations and conditions, to determine the entire range over which these parameters may realistically vary. Each parameter is considered independently, except for the conditioning on wind speed bin; therefore, some improbable or impossible combinations of parameters may arise. The focus here, however, is to get an assessment of how sensitive wind turbine loads are to the variation of these parameters—such that we can decide whether it is appropriate to choose a set value during load calculations or to examine the parameter in greater detail in the future. Future work will examine those parameters that are down-selected as sensitive in order to better understand the dependencies between these parameters.

Some issues were encountered in performing simulations across the ranges of the parameters shown in Table 1. One issue was that some of the coherence matrices generated within Turbsim could not be decomposed (Cholesky factorization failed) for large shear values, α. This issue was addressed by modifying the coherence definition in Eq. 2 to consider the wind speed at the hub height (V_{hub}) rather than the average of the wind speed across the two points (u_m). This correction was determined to be acceptable because velocity spectra are assumed to be constant with height anyway. Another issue encountered was that at extremely negative values of the shear exponent, α, tower blade strikes would often occur. To eliminate this issue, the minimum value of α was changed to -0.75 from -1.5. This change leads to a reduction of the overall range of the parameter, which could potentially lead to a reduced sensitivity. But, multiple studies have shown a large sensitivity of turbine loads to shear value; therefore, we do not believe this reduction in range will lead to a different conclusion.

[‡‡] To avoid numerical issues, u_m was changed to V_{hub}; see Section II.E.

Table 1. Parameter ranges for the three different wind speed bins (below, near, and above rated)

	α	β (*deg*)	L_u (*m*)	L_v (*m*)	L_w (*m*)	σ_u (*m/s*)	σ_v (*m/s*)	σ_w (*m/s*)	a_u	a_v	a_w	b_u	b_v	b_w	γ	PC_{uw} (m^2/s^2)	PC_{uv} (m^2/s^2)	PC_{vw} (m^2/s^2)
Below-rated wind speed, 3-10 m/s																		
Min	-1.5*	-25	5	2	2	0.05	0.02	0.03	1.5	1.7	2	0	0	0	0	-3.5	-4.5	-2.7
Max	3.3	50	1,000	1,000	650	7.2	7.4	4.5	26	18	17	0.08	4.5E-3	0.011	1	0.50	6.0	1.0
Ref.	22	13	6,12	6	6,23	22	22	20,21,22	24	25	12,24	25	20	20	24	21	21	21
Near-rated wind speed, 10-14 m/s																		
Min	-0.4	-10	8	2	2	0.20	0.05	0.05	1.5	1.7	2	0	0	0	0	-3.5	-4.5	-2.7
Max	0.9	50	1,400	1,300	450	7.3	8.1	4.3	26	18	17	0.08	3.0E-3	6.0E-3	1	0.50	6.0	1.0
Ref.	26,24	13,24	6,12	6	6	24,21,22	21,22	20,21,22	24	25	34,24	25	20	20	24	21	21	21
Above-rated wind speed, 14-25 m/s																		
Min	-0.4	-10	25	2	2	0.20	0.18	0.15	1.5	1.7	2	0	0	0	0	-3.5	-4.5	-2.7
Max	0.7	25	1,600	1,500	650	7.4	7.3	4.2	26	18	18	0.05	2.5E-3	6.5E-3	1	0.50	6.0	1.0
Ref.	26,24	13,24	6,25	6	6	20,24,21, 22	21,22	20,21,22	24	25	12,20	25	20	20	24	21	21	21

* This value was changed to -0.75 due to simulation issues

III. Sensitivity Analysis Procedure

Now that the wind parameters of interest have been identified, we need to define a procedure for assessing their sensitivity on the response loads of a wind turbine during operation. A common approach is the calculation of the Sobol sensitivity,[16] which decomponses the variance of the response into fractions that can be attributed to different input parameters and parameter interactions. The drawback of this method is its large computational expense, which requires a Monte Carlo analysis to calculate the sensitivity. To decrease the computational expense, one approach is to use a meta-model, which is a lower-order, surrogate model that is trained on a subset of simulations to act similarly to the original, more computationally expensive model. Some researchers in the wind field have used this approach, [4,6,22,22,] but we are concerned with the complexity of the wind turbine model and associated quantities of interest, especially the system nonlinearities and interaction of the controller for extreme (unlikely) events—and therefore, the ability to accurately represent it with a meta-model. Another approach to reduce computational expense is to use variance-reduction methods to improve the Monte Carlo sampling. Latin hypercube sampling[7,34,35] and fractional factorial analysis[36] are some examples. These methods were considered for this application, but with the large number of parameters being examined, these approaches are still too expensive. Instead, we used a screening method, which provides a sensitivity measure that is not a direct estimate of the variance; rather, it supplies a ranking of those parameters with the most influence. One of the most commonly used screening approaches is called Elementary Effects analysis.[37-43]

A. Overview of Elementary Effects

Elementary Effects (EE) at its core is a very simple methodology for screening parameters. It is based on the one-at-a-time approach in that each parameter of interest is varied individually while holding all other parameters fixed. A derivative is then calculated based on the level of change in the response of interest to the change in the input parameter. Approaches such as these are called local-sensitivity approaches because they only calculate the influence of a single parameter, and they do not consider how the other parameters interact with the response. But, EE extends this process by examining the change in response for a given input parameter at different locations in the input parameter hyperspace. In other words, only one parameter is varied at a time, but this variation is performed multiple times using different values for the other input parameters. The derivatives calculated from these different points are then averaged to assess an overall level of sensitivity. Thus, the EE method considers the interactions between different parameters and is therefore considered a global sensitivity analysis method.

The basic approach for performing an EE analysis has been modified over the years to ensure that the input hyperspace is being adequately sampled and to eliminate issues that might confound the sensitivity assessment. In this work, we have chosen to use 1) Sobol random numbers to determine the initial points at which the derivatives will be calculated, which ensures a wide sampling of the input hyperspace, and 2) a radial approach rather than the traditional trajectories for varying all of the parameters, which has been shown to improve the efficiency of the method.[44]

We are interested in understanding the sensitivity of a response load of a wind turbine, Y, to different characteristics of the wind, X (matrix of input parameters):

$$Y = f(X_1, X_2, X_3, ...X_k), \tag{3}$$

where k is the total number of input parameters (in this case k = 18). All input parameters are normalized between zero (their minimum value) and one (their maximum value).

For a given sampling of **X**, (x_1, x_2, …, x_k), the elementary effect of the i^{th} input parameter is found by varying only that parameter by a normalized amount Δ:

$$EE_i = \frac{Y(x_1, ..., x_{i-1}, x_i + \Delta, x_{i+1}, ..., x_k) - Y(x_1, x_2, ..., x_k)}{\Delta}. \tag{4}$$

Typically, Δ is kept the same for each parameter, but a variable value can also be used, as discussed later in this section. Because of the normalization of **X**, the elementary effect (EE_i) can be thought of as the local partial derivative of the output (Y) with respect to the input (x_i) multiplied by the total maximum-to-minimum range of the input. Thus, the elementary effect has the same units as the output.

In a radial sensitivity approach, *EE* is calculated for each of the parameters for a given sample point by varying each of the parameters individually from that point. (This is different than the original EE methodology, which creates a trajectory by varying each new parameter from the Δ point of the previous parameter.) This process is repeated for r starting points in the input parameter hyperspace, creating a set of r-different calculations of *EE* for each parameter.

The overall influence of a parameter, i, is then estimated as the mean of the absolute value of the elementary effects at the r different locations:

$$\mu_i^* = \frac{1}{r}\sum_{j=1}^{r}\left|EE_i^j\right|. \tag{5}$$

In addition, the interaction effects from other input parameters is estimated as the standard deviation of the individual *EE* estimates:

$$\sigma_i = \sqrt{\frac{1}{(r-1)}\sum_{j=1}^{r}(EE_i^j - \mu_i)^2}, \tag{6}$$

where μ_i is the mean of the elementary effects without the absolute value taken.

There are many different ways to choose the starting points at which *EE* is calculated. The original approach was to use a random sampling; however, this does not ensure a good coverage of the input hyperspace. Another approach involves using Latin hypercube sampling, and Campolongo et al.[45] suggest using Sobol quasi-random numbers instead. We initially chose to use the Campolongo approach, which generates a quasi-random matrix of Sobol numbers of size (r+4,2k) from which the first four rows of the right half of the matrix are discarded (and the remaining rows shifted up). The left half of the first r rows are then used as the r different starting locations for the *EE* calculation. The second half of each of these rows defines the auxiliary value ot which each parameter should be changed, individually, from the initial starting point on the left half of the row. The Sobol numbers are values between 0 and 1 that indicate the normalized value of each input to use. In this approach, the parameters are not being varied by the same amount every time to calculate *EE*, which adds to the robustness of the method. An example of the Sobol quasi-random sequence is given in Table 2, showing the first eight points of a 10-dimensional sequence. Table 3 then shows how to use this sequence to generate the starting and auxiliary points for an example problem with five inputs (k) and eight radial points (r), based on the description above of shifting the right half of the matrix up by four rows, and retaining only the first eight rows of the left half of the matrix.

However, we encountered issues using this approach. In this study, there are many parameters of interest, and we therefore need many different evaluation points to obtain a good assessment of their overall sensitivity. When using the Campolongo approach for the *EE* evaluation with a value of r = 20 points and k = 18 parameters, we found that some of the auxiliary points and starting points were the same—thus creating a zero delta (no change). We attempted to shift the rows and use other parts of the Sobol sequence, but this issue persisted. We also found that some of the delta values in this approach were very small; therefore, the derivatives would sometimes become extremely large due to numerical innacuracies. So we decided to retain the Sobol starting points, but choose the auxiliary points based on a random selection of delta values between -1 and 1. Difficulties arose from this approach as well, because we found that some of the parameter combinations at the extreme edges led to extreme, unnatural

loading conditions that the simulations could not resolve. In addition, when a large delta value is used, the derivative calculated is assuming a linear relationship over a very large parameter range, which could be very innacurate and lead to incorrect sensitivity assessments.

Therefore, the final approach chosen for this work was to continue to use the Sobol quasi-random sequence for the starting points (as shown in Table 2), but then use only random selections of -0.1 and 0.1 for the deltas, from which the auxiliary points are defined and the associated derivatives calculated. This approach allows us to still sample a significant part of the hyper-parameter space, but calculate the sensitivities of the parameters in those locations in a manner that is consistent with the linear assumptions and that also does not create numerical issues. A delta of magnitude 0.1—i.e., 10% of the total maximum-to-minimum range—is expected to be a good compromise in terms of not too small to avoid numerical issues and not too large to smooth out nonlinearities.

Table 2. 10-dimensional Sobol quasi-random sequence, first 12 points

0.5000	0.5000	0.5000	0.5000	0.5000	0.5000	0.5000	0.5000	0.5000	0.5000
0.2500	0.7500	0.2500	0.7500	0.2500	0.7500	0.2500	0.7500	0.7500	0.2500
0.7500	0.2500	0.7500	0.2500	0.7500	0.2500	0.7500	0.2500	0.2500	0.7500
0.1250	0.6250	0.8750	0.8750	0.6250	0.1250	0.3750	0.3750	0.8750	0.6250
0.6250	0.1250	0.3750	0.3750	0.1250	0.6250	0.8750	0.8750	0.3750	0.1250
0.3750	0.3750	0.6250	0.1250	0.8750	0.8750	0.1250	0.6250	0.1250	0.8750
0.8750	0.8750	0.1250	0.6250	0.3750	0.3750	0.6250	0.1250	0.6250	0.3750
0.0625	0.9375	0.6875	0.4375	0.8125	0.0625	0.4375	0.5625	0.8125	0.6875
0.5625	0.4375	0.1875	0.9375	0.3125	0.5625	0.9375	0.0625	0.3125	0.1875
0.3125	0.1875	0.9375	0.6875	0.5625	0.8125	0.1875	0.3125	0.0625	0.9375
0.8125	0.6875	0.4375	0.1875	0.0625	0.3125	0.6875	0.8125	0.5625	0.4375
0.1875	0.3125	0.3125	0.5625	0.4375	0.1875	0.0625	0.9375	0.1875	0.0625

Table 3. Elementary Effects sample points for *k*=5, *r*=8. Left half of matrix are the starting points and right half are the auxiliary points.

0.5000	0.5000	0.5000	0.5000	0.5000	0.6250	0.8750	0.8750	0.3750	0.1250
0.2500	0.7500	0.2500	0.7500	0.2500	0.8750	0.1250	0.6250	0.1250	0.8750
0.7500	0.2500	0.7500	0.2500	0.7500	0.3750	0.6250	0.1250	0.6250	0.3750
0.1250	0.6250	0.8750	0.8750	0.6250	0.0625	0.4375	0.5625	0.8125	0.6875
0.6250	0.1250	0.3750	0.3750	0.1250	0.5625	0.9375	0.0625	0.3125	0.1875
0.3750	0.3750	0.6250	0.1250	0.8750	0.8125	0.1875	0.3125	0.0625	0.9375
0.8750	0.8750	0.1250	0.6250	0.3750	0.3125	0.6875	0.8125	0.5625	0.4375
0.0625	0.9375	0.6875	0.4375	0.8125	0.1875	0.0625	0.9375	0.1875	0.0625

B. Assessment of Sensitivity

The EE method enables the screening of the most sensitive parameters by examining μ_i^* and σ_i. But, with increasing sample points (*r*), the EE method can also provide an estimation of the global sensitivity. Campolongo et al.[45] suggest using an estimator introduced by Jansen:[46]

$$E_{\mathrm{X}:i}\left(V_{X_i}(Y\mid \mathrm{X}_{:i})\right)=\frac{1}{2r}\sum_{j=1}^{r}\left(y(a_1^{(j)},a_2^{(j)},\ldots a_k^{(j)})-y(a_1^{(j)},a_2^{(j)},\ldots,b_i^{(j)},\ldots,a_k^{(j)})\right)^2, \quad (7)$$

where $\mathbf{a}^{(j)}$ is the j^{th} starting point, $\mathbf{b}^{(j)}$ is th j^{th} auxiliary point, $\mathrm{X}_{:i}$ is the matrix of all variables but X_i, $V_{X_i}(Y\mid \mathrm{X}_{:i})$ is the inner variance, *V*, of *Y* taken over all possible values of X_i while keeping $\mathrm{X}_{:i}$ fixed, and $E_{\mathrm{X}:i}$ is the output expectation taken over all possible values $\mathrm{X}_{:i}$

IV. Approach Implemented

The following sections describe in more detail the steps of how the Elementary Effects analysis was accomplished for our application.

A. Wind Turbine Model and Tools

To examine the sensitivity of each wind parameter on turbine response loads, we need to simulate a wind turbine model. We used the NREL 5-MW reference turbine,[47] which is a variable-speed, 3-bladed, upwind, horizontal-axis turbine with a hub height of 90 m and a rotor diameter of 126 m. By repeating this analysis with other wind turbine models, future work could examine how the sensititivity of the parameters on turbine loads is affected by the size of wind turbine considered.

For each of the parameter settings identified with the Elemetary Effects procedure, 30 different turbulent wind files (i.e. 30 independent time-domain realizations from 30 seeds) are generated in TurbSim.[20] Analysis showed that 30 wind seeds were needed to get converged statistics for the response of the turbine. A 25 x 25 square grid is used that covers the entire rotor plane of the turbine. The aero-servo-elastic tool, FAST (v8), is then used to simulate a model of the NREL 5-MW wind turbine using the wind files developed. Aerodynamic drag on the tower is not considered because it will be minimal for an operational turbine. BeamDyn, the new module in FAST that allows for a finite-element description of the blades, is also not used because the NREL 5-MW turbine does not have the level of structural flexibility that warrants a model of this type. Otherwise, all normal aero-servo-elastic features of FAST v8 are enabled, including quasi-steady induction, unsteady airfoil aerodynamics; blade, drivetrain, and tower structural flexibility; and an active variable-speed and rotor-collective blade-pitch-to-feather controller.

B. Quantities of Interest

From the output of the simulations, quantities of interest (QoI) are extracted that capture the variability of the turbine response. The QoI chosen for this work are summarized in Table 4 and include the blade, drivetrain, and tower loads, as well as the blade-tip displacement and turbine power output. Both the ultimate and fatigue loads are considered. The ultimate loads are estimated using the average of the global absolute maximums across all turbulence seeds for a given set of parameter values, whereas the fatigue loads are estimated using the average of the standard deviations of the output response across all seeds for a given set of parameter values. For the bending moments, the ultimate loads are calculated as the largest vector sum of the first two components listed, rather than considering each individually.

Table 4. Quantities of interest to be examined in sensitivity analysis

Quantity of Interest	Component		
Blade-root moments	Out-of-plane bending	In-plane bending	Pitching moment
Low-speed shaft moments at main bearing	0-degree bending	90-degree bending	Shaft torque
Tower-top moment	Fore/aft bending	Side/side bending	Yaw moment
Tower-base moment	Fore/aft bending	Side/side bending	
Out-of-plane blade-tip displacement	Just for ultimate		
Electrical power			

C. Sensitivity Analysis

The wind turbine parameter settings for each simulation are prescribed by the Elementary Effects approach. For our analysis, we are examining 18 parameters (k), and we have chosen to initially use 20 different starting points (r). The choice of the number of starting points is subjective; a high number was chosen in hopes of capturing a good estimate of the sensitivity of each parameter. However, examination of the convergence of the sensitivity showed that more points were needed, and so, a total of 30 points were used in this analysis. Additionally, 30 different turbulence seeds (s) are simulated for each parameter space sampling, and the sensitivity analysis is conducted for each of the three wind speed bins (ws). Thus, the total number of simulations performed is $r*(k+1)*s*ws$ = 30*19*30*3 = 51,300, with a simulation time of 10 minutes each (after 30 s of start-up transient time is removed).

A different turbulent wind file is generated for each of these simulations, using a sampling of the different wind parameters prescribed by the EE procedure introduced above. The remainder of the settings are the same for each simulation, with the exception of the mean wind speed for the three bins, and the associated initial rotor speed and pitch settings. For each QoI, the elementary effects of the input parameters is calculated (Eq. 4), along with the mean (Eq. 5) and standard deviation (Eq. 6) of the elementary effects across each of the radial points evaluated.

V. Results

The results of the sensitivity analysis are summarized through plots of the standard deviation of the elementary effects calculated at the 30 different Sobol point locations against the mean of the elementary effects across those same points. The mean value indicates the sensitivity of a parameter, whereas the standard deviation shows the variability in the sensitivity to the value of the parameter, as well as the interaction effects of the other parameters. Plotted together, sensitive parameters are identified as those with high mean and/or high standard deviation (those outside the lower-left quadrant of each plot). In Figures 2 to 9 of the appendix, these sensitivity plots have been created for each wind speed bin, for both ultimate and fatigue loads, and for the 13 outputs summarized in Table 4. Figure 1 provides an example histogram of the values for three of the parameters, associated with the absolute ultimate blade root pitching moment (from which μ_i^* is derived; σ_i is derived from the histogram without the absolute value).

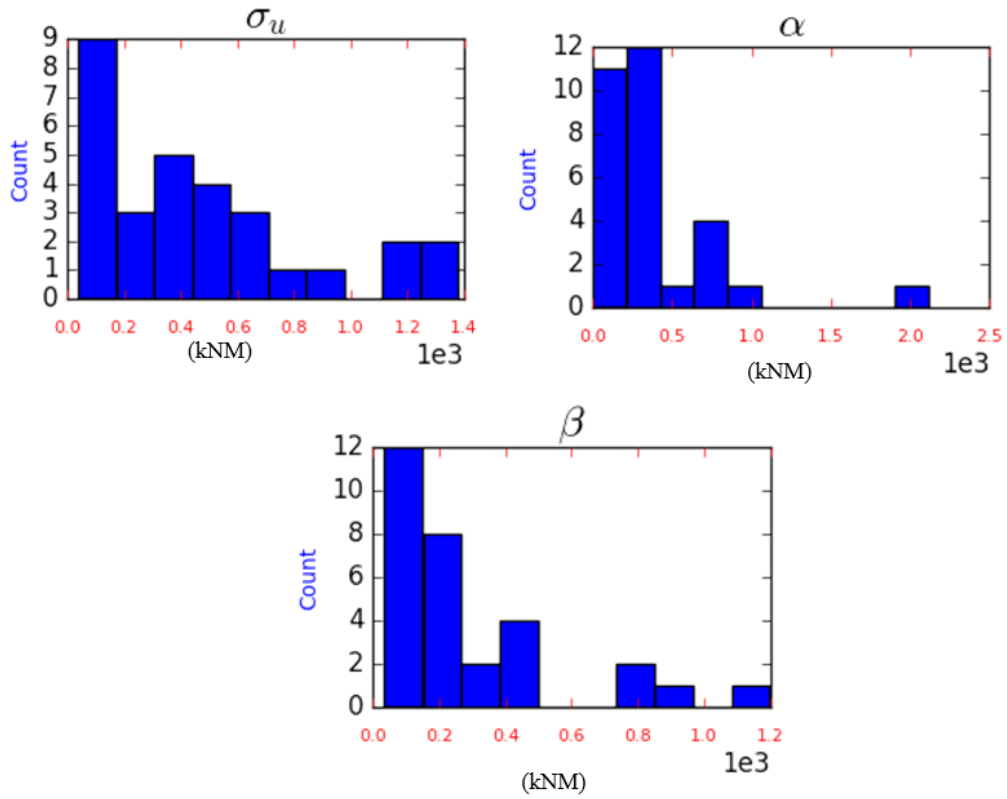

Figure 1. Histograms of absolute values of elementary effects of top three parameters on ultimate blade-root pitching moments in BIN-1

Note that some issues were encountered for some of the simulation cases. First, one of the Sobol points in wind speed bin 3 had persistent issues with the coherence decomposition. Ultimately, we chose to remove this point from evaluation, hence decreasing the number of points in wind bin 3 to 29 instead of the 30 original points. Additional issues were found for some of the simulations within wind speed bins 2 and 3 under high shear related to excessive excitation of the edgewise bending of the blades and poor controller performance. More research is needed to understand and eliminate this issue; but in this paper, these simulation cases were simply removed in assessing the sensitivity of α, resulting in a total of 30 Sobol points considered for wind speed bin 1, 23 for wind speed bin 2, and 22 for wind speed bin 3. This point is very important, since before we removed these simulation cases, instabilities in the rotor response were creating very different levels of sensitivities for some parameters—showing the need to thoroughly assess the output results being evaluated.

Tables 5 summarizes the top three most sensitive parameters (from right to left using data outside the lower-left quadrant) for each of the sensitivity plots given in Figures 2 to 9. Table 6 then summarizes the total number of times that a given parameter is identified as sensitive (outside the lower-left quadrant) across all wind speed bins, outputs, and for both fatigue and ultimate loads. It is obvious that, overall, the shear exponent (***α***) is the most sensitive

parameter across nearly all outputs, and for both ultimate and fatigue load values. The second most sensitive parameter is the turbulence standard deviation in the primary wind propogation direction (u-direction), σ_u. The high sensitivities of these two parameters are expected and are consistent with the findings of other researchers and their importance in wind turbine design standards. Beyond these two parameters, however, there are parameters that show a secondary level of significance that varies across the different outputs. For those outputs associated with the u-direction of the wind, we see that the parameters associated with the coherence model in the u-direction tend to dominate at the secondary level, which includes the a_u and b_u parameters. Wind veer, β, also shows a noticeable level of significance at times.

Table 5. Ranking of top parameters identified for each quantity of interest

Quantities of Interest	BIN-1 Ranking			BIN-2 Ranking			BIN-3 Ranking		
	1	2	3	1	2	3	1	2	3
I. Blade loads									
Ultimate loads									
Blade-root bending moment	α	-	-	α	-	-	α	-	-
Blade-root pitching moment	σ_u	α	β	σ_u	α	L_u	σ_u	b_w	γ
Blade-tip out of plane deflection	α	-	-	α	-	-	α	b_u	-
Fatigue loads									
Blade-root bending moment (in-plane)	-	-	-	-	-	-	α	-	-
Blade-root bending moment (out-of-plane)	-	-	-	α	-	-	α	-	-
Blade-root pitching moment	-	-	-	-	-	-	α	-	-
II.Drivetrain loads									
Ultimate loads									
Main shaft bending moment	α	-	-	α	-	-	α	-	-
Rotor torque	α	σ_u	-	-	-	-	σ_u	b_w	b_v
Fatigue loads									
Main shaft bending moment (0º)	-	-	-	α	-	-	α	-	-
Main shaft bending moment (90º)	-	-	-	α	-	-	α	-	-
Rotor torque	σ_u	α	b_u	α	σ_u	b_u	σ_u	α	-
III. Tower loads									
Ultimate loads									
Tower-top bending moment	-	-	-	α	-	-	α	-	-
Tower-top yaw moment	σ_u	α	-	α	σ_u	-	α	σ_u	b_u
Tower-base bending moment	σ_u	α	-	α		-	b_u	σ_u	α
Fatigue loads									
Tower-top bending(fore-aft) moment	σ_u	α	b_u	α	σ_u	b_u	σ_u	-	-
Tower-top bending (side-side) moment	σ_u	α	-	σ_u	-	-	σ_u	β	b_u
Tower-top yaw moment	σ_u	-	-	σ_u	-	-	σ_u	b_u	β
Tower-base bending(fore-aft) moment	-	-	-	-	-	-	σ_u	L_u	b_u
Tower-base bending (side-side) moment	α	σ_u	-	σ_u	α	-	b_u	σ_u	L_u
IV. Electrical power									
Ultimate									
Electrical power	α	-	-	-	-	-	-	-	-
Fatigue									
Electrical power	α	b_u	a_u	α	b_u	β	-	-	-

No significant levels of sensitivity—except for the blade-root ultimate pitching moment and rotor torque—are noted for the cross-correlation components between the turbulence in different directions at a given point (*PC*), the integral length scale, or the off-axis (v and w) components of the turbulence and coherence. However, the strong

sensitivity of the two largest parameters (especially shear) could mask the levels of sensitivity of some of these other parameters. So a useful next step could be to re-run these simulations at a fixed value of shear and turbulence intensity in the *u*-direction to more closely examine the sensitivity of the other parameters without the overriding influence of shear and σ_u

In general, the sensitivity ranges for both the ultimate and fatigue loads increase with increasing wind speed bin. The exception to this trend is electrical power, in which the highest wind speed bin has the lowest levels of sensitivity (due to the regulation of power by the controller).

To ensure the significance of a parameter, we also need to make sure that the sensitivity estimates have sufficiently converged. Although the elementary effects is not a true sensitivity value, the mean of the elementary effects is an indicator of the sensitivity, and Equation 7 provides a sensitivity estimate. Figures 10 and 11 (in the Appendix) show the convergence rate of both the *EE* mean and sensitivity estimate for the blade-root ultimate pitching moment and rotor torque fatigue, across the top three most sensitive parameters. In general, we see a very similar rate of convergence for these two different metrics. These convergence plots help us understand whether more simulations may be warranted. It has been shown that the radial point method, as used in this paper, has a good convergence rate compared to other *EE* analysis methods. Initially, 20 points were chosen for this analysis, and we had to increase the number to 30 due to the lack of convergence. Even now, many of the parameters can still be considered unconverged. However, with the large levels of separation in sensitivity between shear and *u*-direction turbulence level as compared to the remainder of the parameters, there is little doubt that these two parameters are the most significant. Further analysis by adding more simulations, or removing shear and *u*-turbulence variability, would be useful to better understand the relative level of sensitivity of the secondary parameters identified.

Table 6. Number of appearances of parameters identified for each wind speed bin

Parameters	BIN-1		BIN-2		BIN-3		Total appearances	
	Ultimate loads	Fatigue loads	Ultimate loads	Fatigue loads	Ultimate loads	Fatigue loads	**Ultimate loads**	**Fatigue loads**
$\boldsymbol{\alpha}$	*8*	*5*	*7*	*7*	*6*	*7*	***21***	***19***
$\boldsymbol{\beta}$	*1*	*2*	-	*1*	*2*	*4*	***3***	***7***
$\boldsymbol{L_u}$	-	-	-	-	*1*	*2*	***1***	***2***
L_v	-	-	-	-	-	-	***0***	***0***
L_w	-	-	-	-	-	-	***0***	***0***
$\boldsymbol{\sigma_u}$	*4*	*6*	*2*	*5*	*4*	*6*	***10***	***17***
σ_v	-	-	-	-	-	-	***0***	***0***
σ_w	-	-	-	-	-	-	***0***	***0***
$\boldsymbol{a_u}$	-	*3*	-	*1*	*1*	*2*	***1***	***6***
a_v	-	-	-	-	-	-	***0***	***0***
a_w	-	-	-	-	-	-	***0***	***0***
$\boldsymbol{b_u}$	-	*3*	-	*3*	*3*	*4*	***3***	***10***
b_v	-	-	-	-	*2*	-	***2***	***0***
b_w	-	-	-	-	*2*	-	***2***	***0***
γ	-	-	-	-	*2*	*1*	***2***	***1***
PC_{uw}	-	-	-	-	*2*	-	***2***	***0***
PC_{uv}	-	-	-	-	*2*	-	***2***	***0***
PC_{vw}	-	-	-	-	*2*	-	***2***	***0***

VI. Conclusions

As described in this paper, we performed a screening analysis of the most sensitive wind parameters to the resulting loads and power performance for the representative NREL 5-MW wind turbine. The study did not consider specific site conditions, but rather, focused on understanding the most sensitive parameters across the range of possible values for a variety of sites. To limit the number of simulations required, we used a screening analysis using elementary effects, instead of a more computationally intensive sensitivity analysis. Elementery effects are an assessment of the local sensitivity of a parameter at a given location in space through variation of only that parameter, averaged over multiple points throughought the parameter hyperspace. To speed convergence, we applied a modification of the standard elementary effects approach using radial points, but with set delta values of

+/- 0.1. The elementary effects were shown to give similar values to an approximation of the sensitivity, but many points were needed to get to a reasonable level of convergence.

The purpose of this exercise was to assess the sensitivity of different wind parameters on the resulting loads of the wind turbine, to 1) rank the sensitivities of different parameters, 2) help establish error bars around predictions of engineering models during validation efforts, and 3) provide insight to probabilistic design methods and site-suitability analyses. This study shows that the loads and power are highly sensitive to the shear and turbulence levels in the *u*-direction—and, to a lesser extent, the coherence parameters in the *u*-direction as well as veer. Items (2) and (3) are left for future work.

The combinations of parameters in this study spanned the ranges of several different locations. However, the parameters were considered independent of one another, which likely resulted in non-physical wind scenarios. The screening analysis, though, has shown us which parameters are most important to examine in more detail in future work.

Appendix

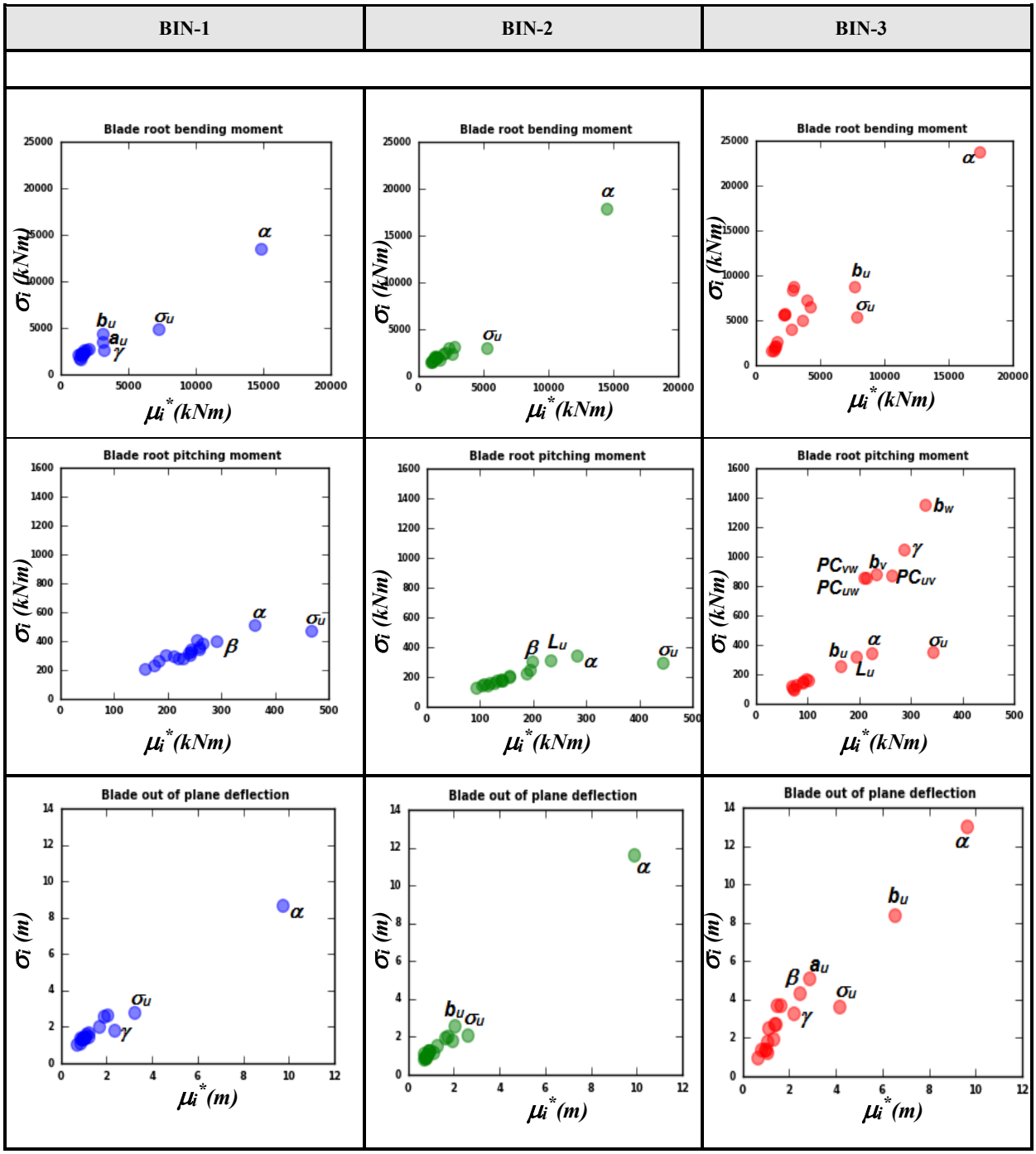

Figure 2. Elementary effects for blade ultimate loads: mean (μ_i^*) versus standard deviation (σ_i^*).

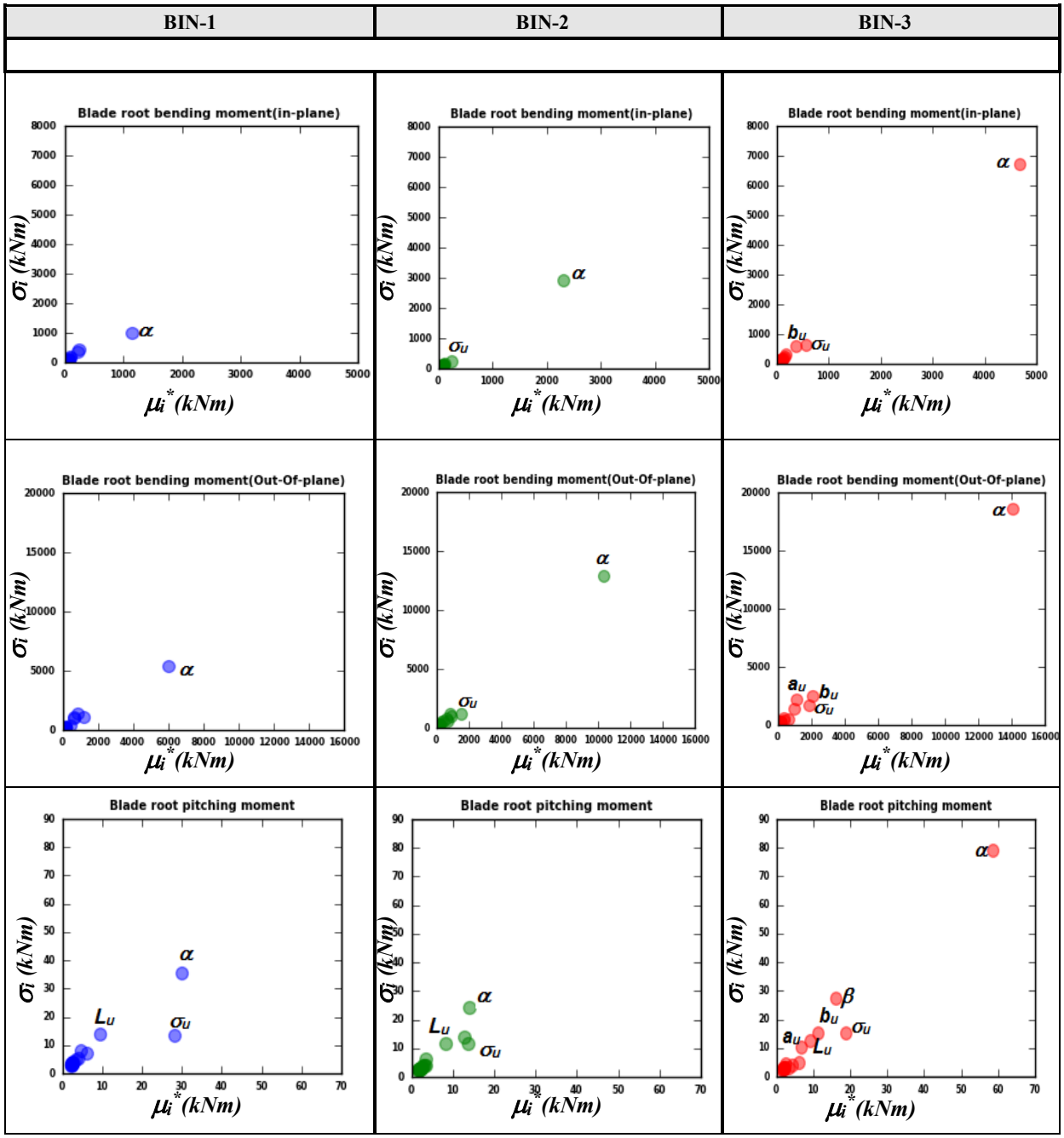

Figure 3. Elementary effects for blade fatigue loads: mean (μ_i^*) versus standard deviation (σ_i^*).

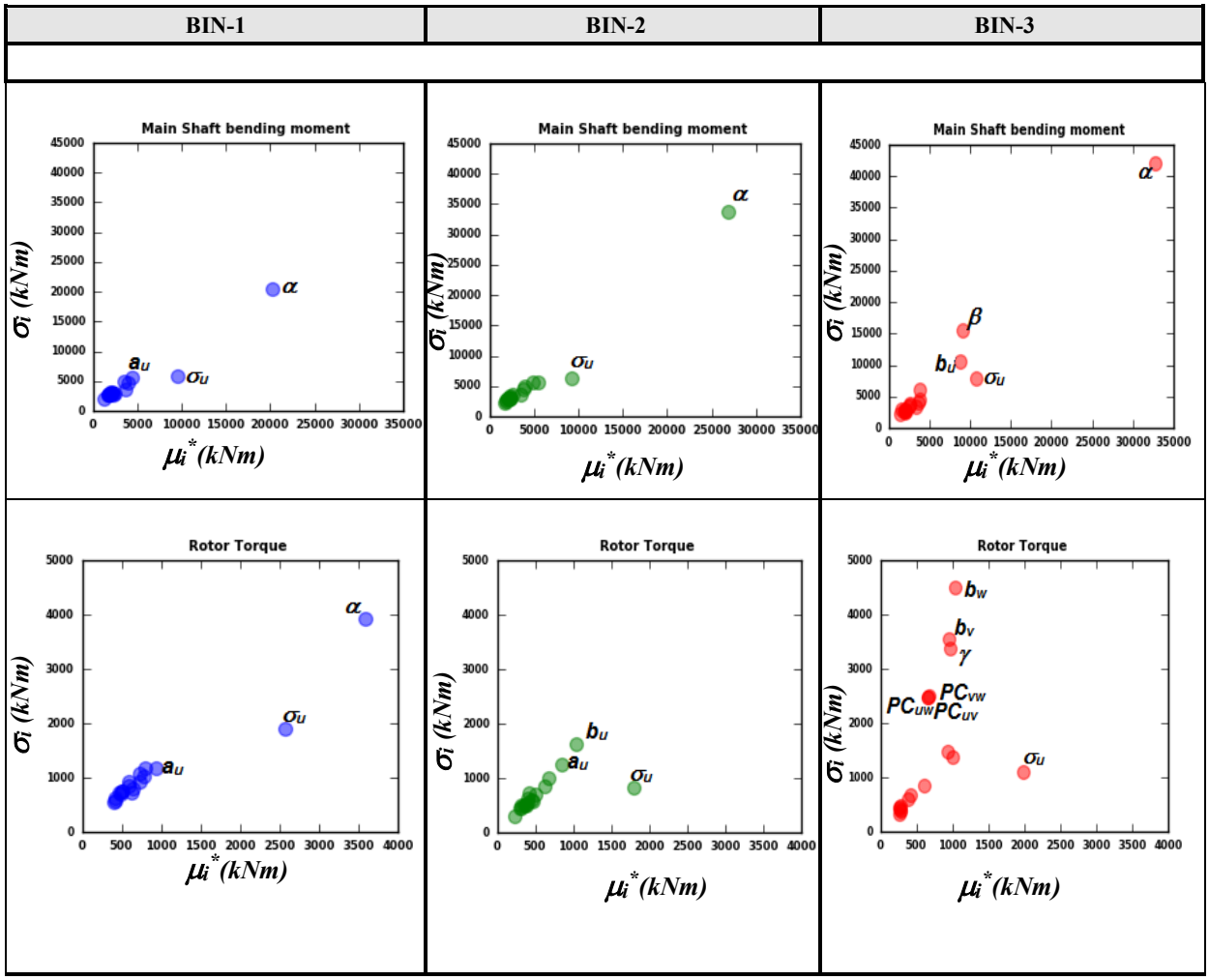

Figure 4. Elementary effects for drivetrain ultimate loads: mean (μ_i^*) versus standard deviation (σ_i^*).

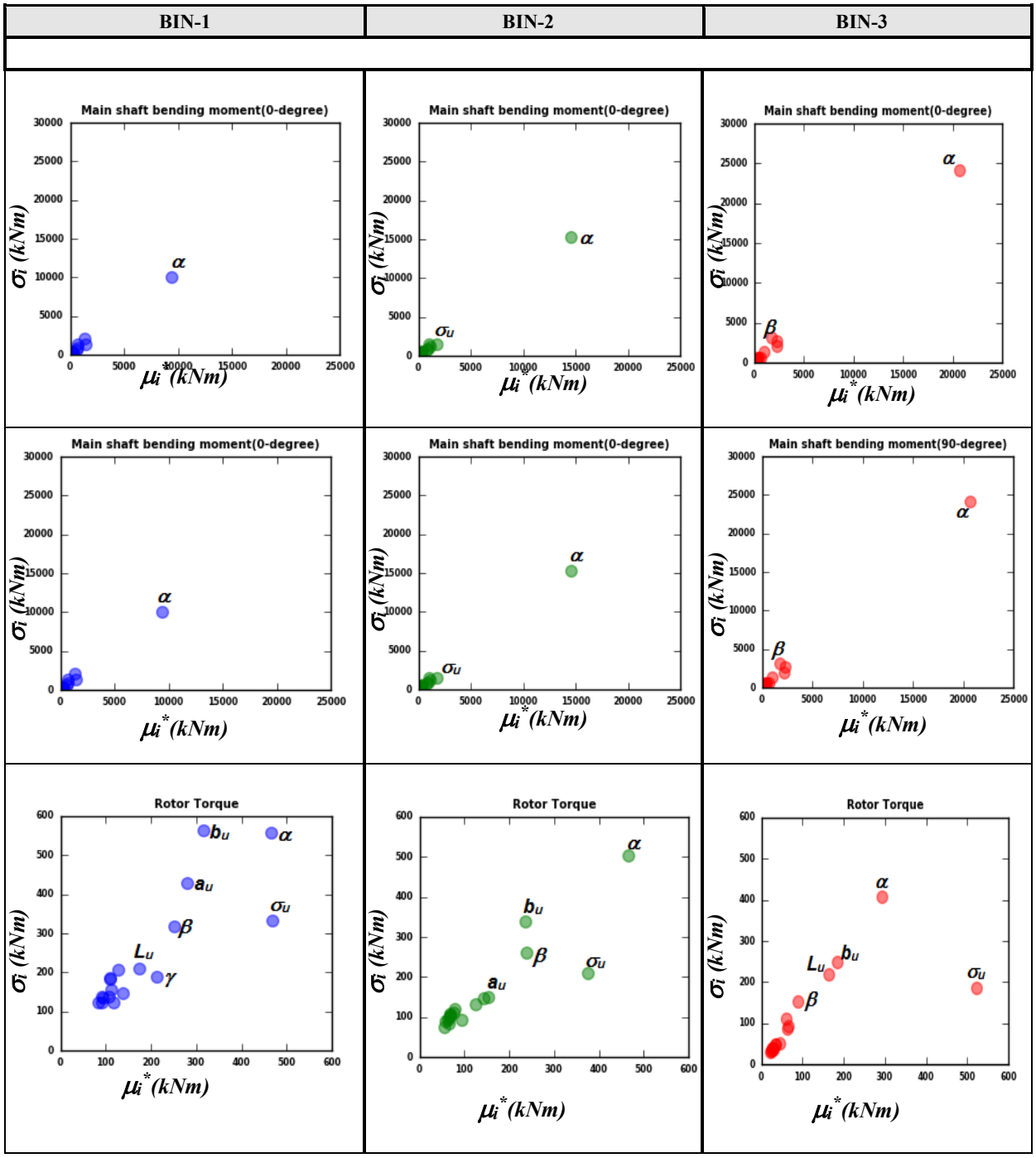

Figure 5. Elementary effects for drivetrain fatigue loads: mean (μ_i^*) versus standard deviation (σ_i^*).

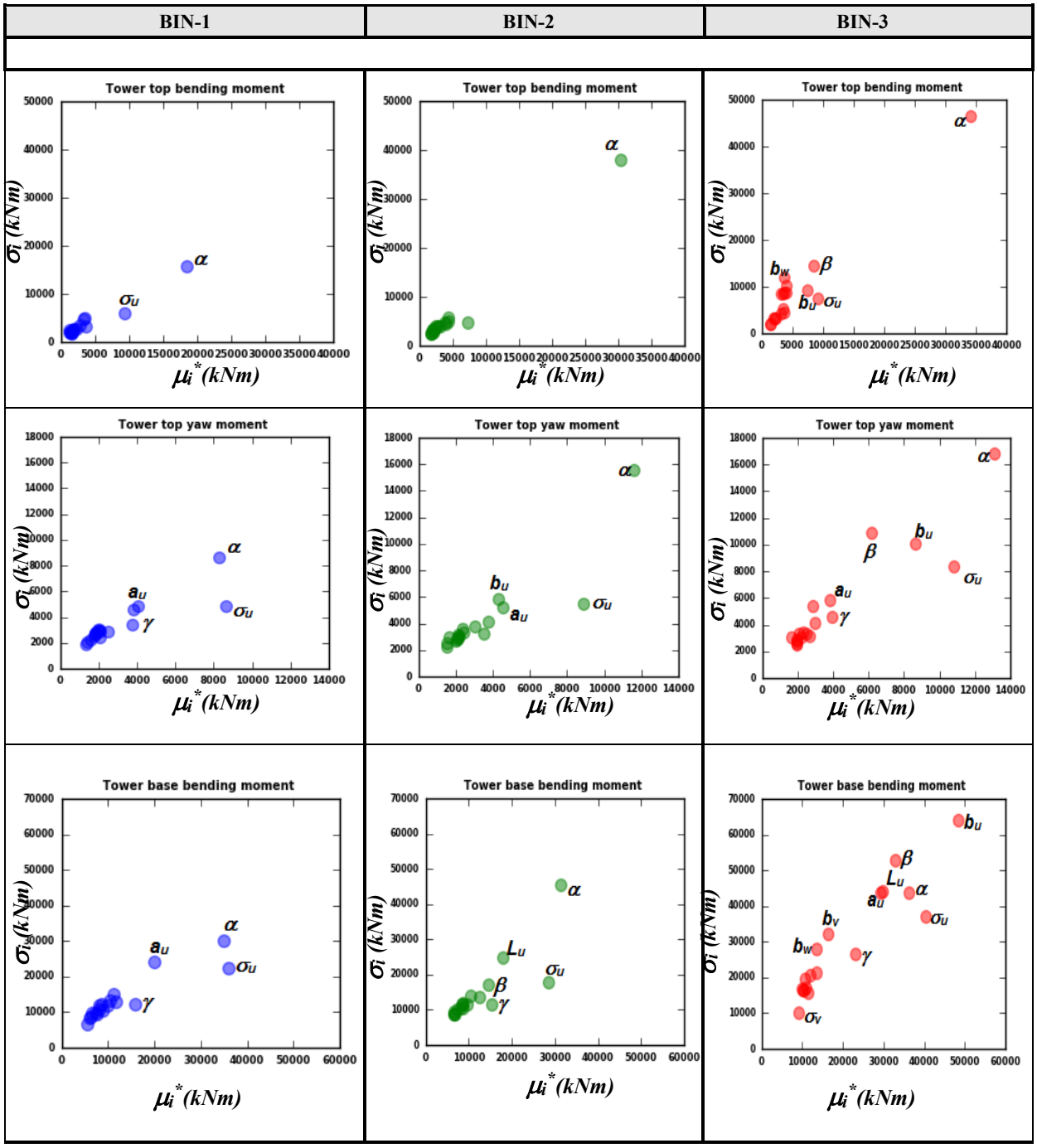

Figure 6. Elementary effects for tower ultimate loads: mean (μ_i^*) versus standard deviation (σ_i^*).

BIN-1	BIN-2	BIN-3
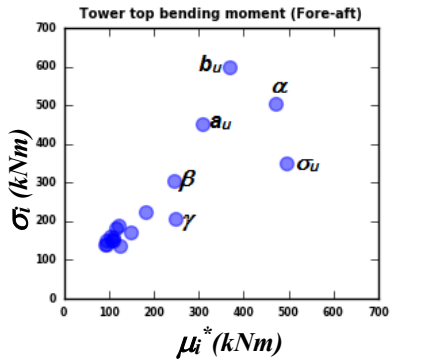	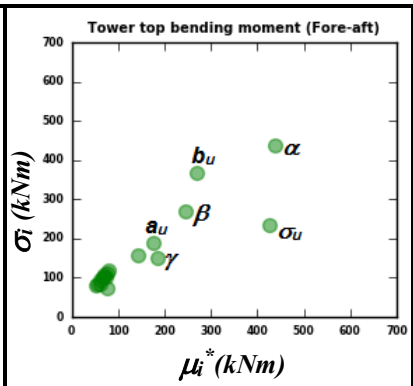	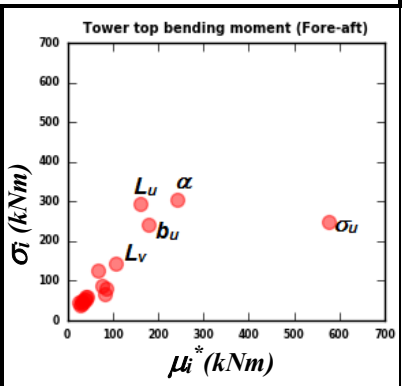
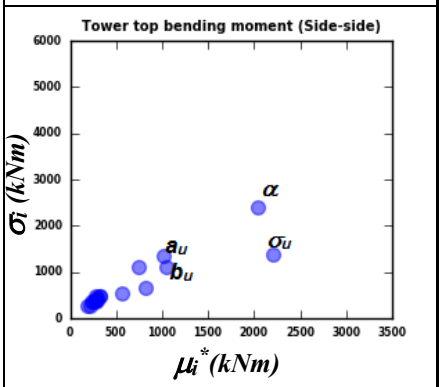	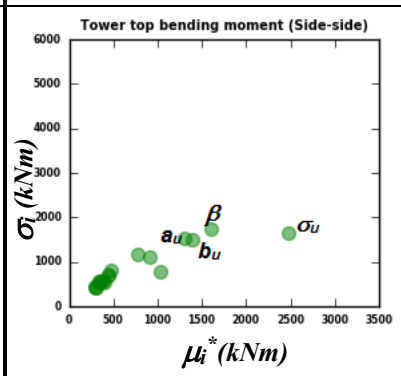	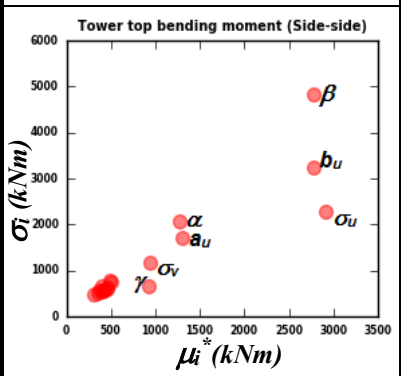
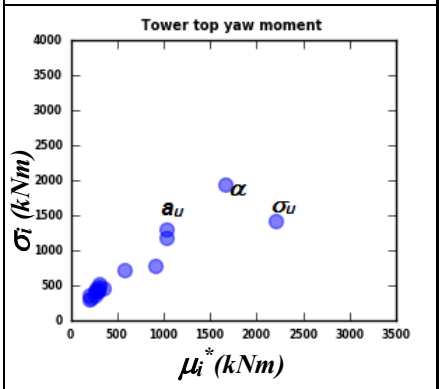	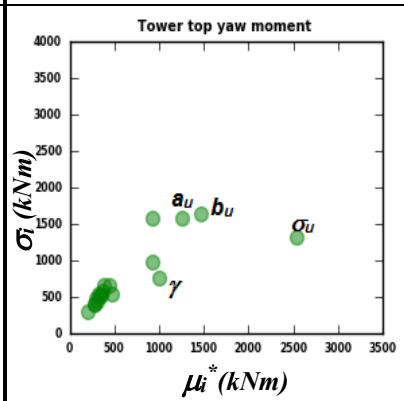	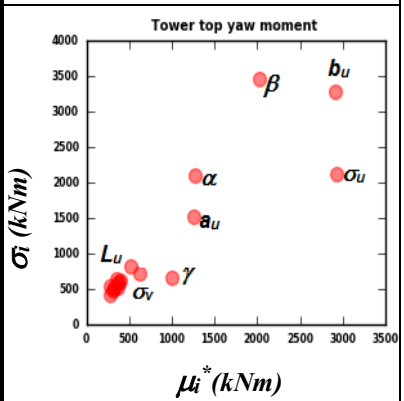
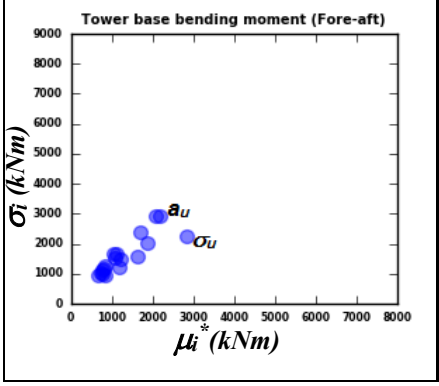	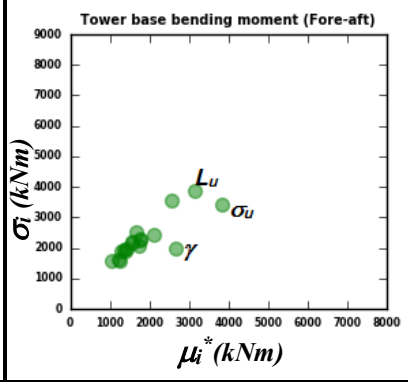	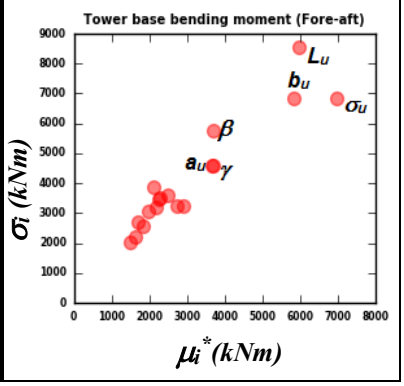

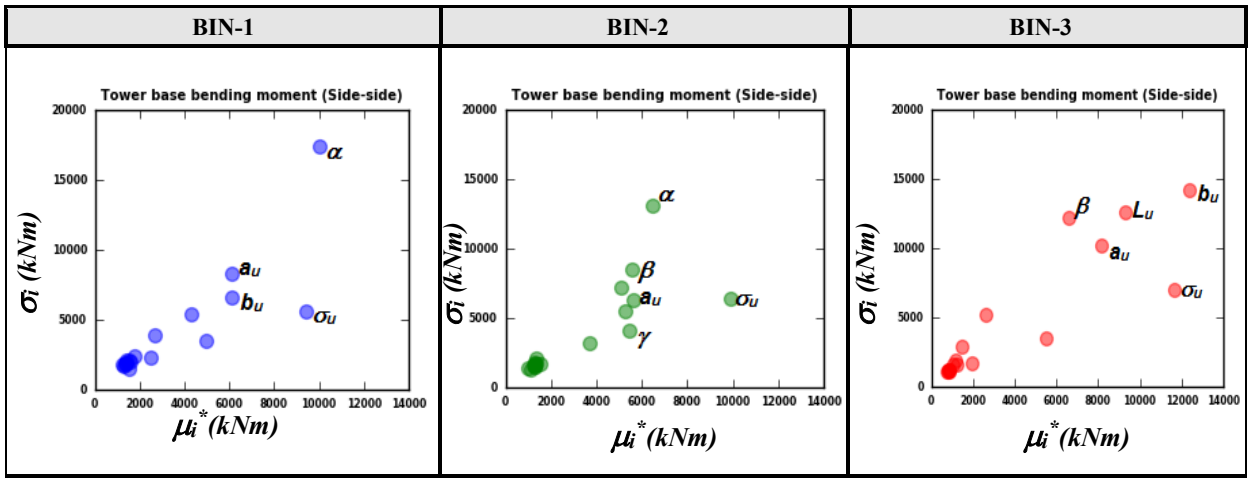

Figure 7. Elementary effects for tower fatigue loads: mean (μ_i^*) versus standard deviation (σ_i^*).

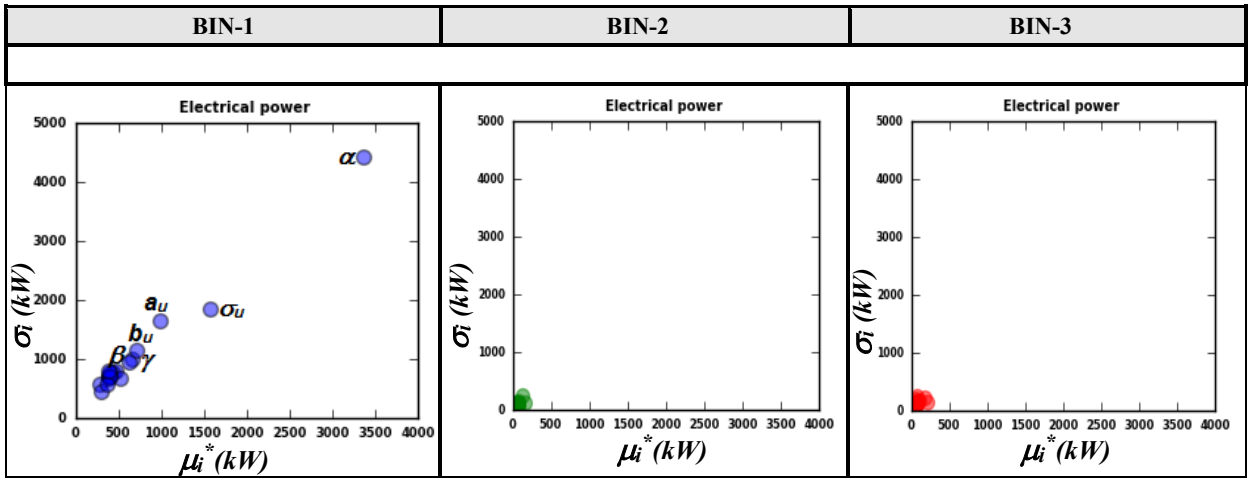

Figure 8. Elementary effects for extreme electrical power: mean(μ_i^*) versus standard deviation (σ_i^*).

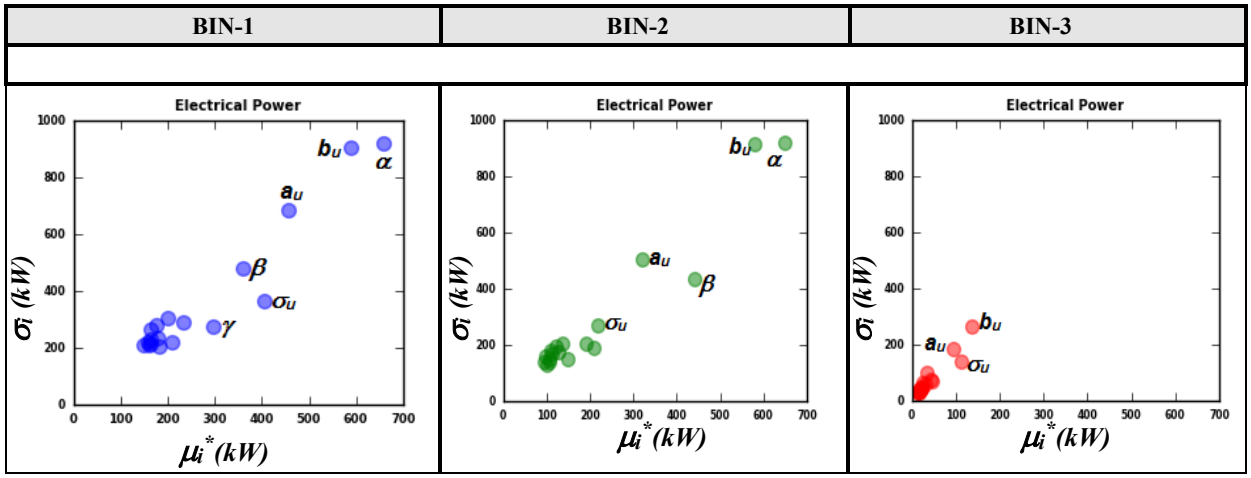

Figure 9. Elementary effects for standard deviation of electrical power: mean (μ_i^*) versus standard deviation (σ_i^*).

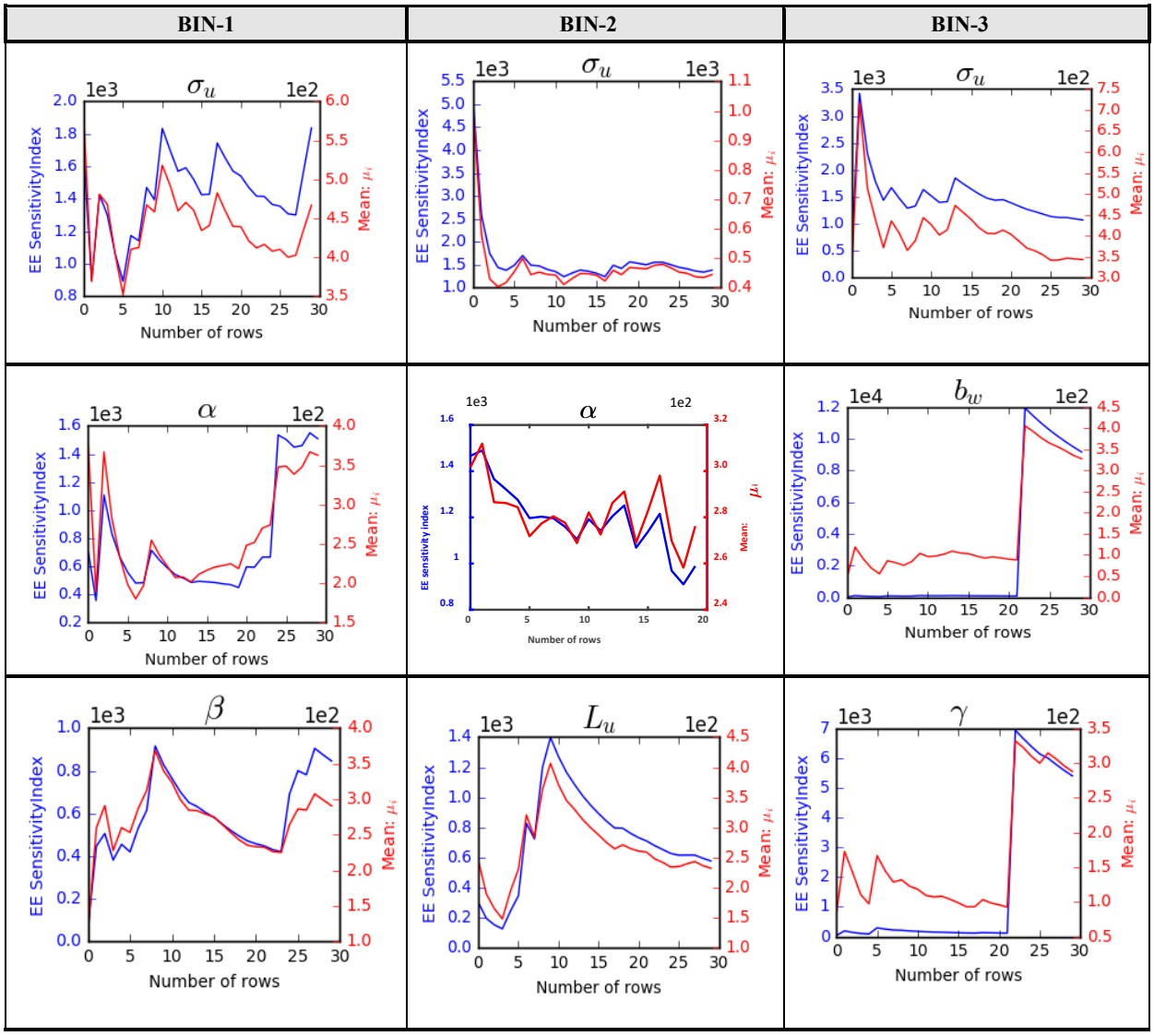

Figure 10. Elementary effects convergence for the top three sensitive parameters identified for ultimate blade-root pitching moment: mean (μ_i^*) and sensitivity.

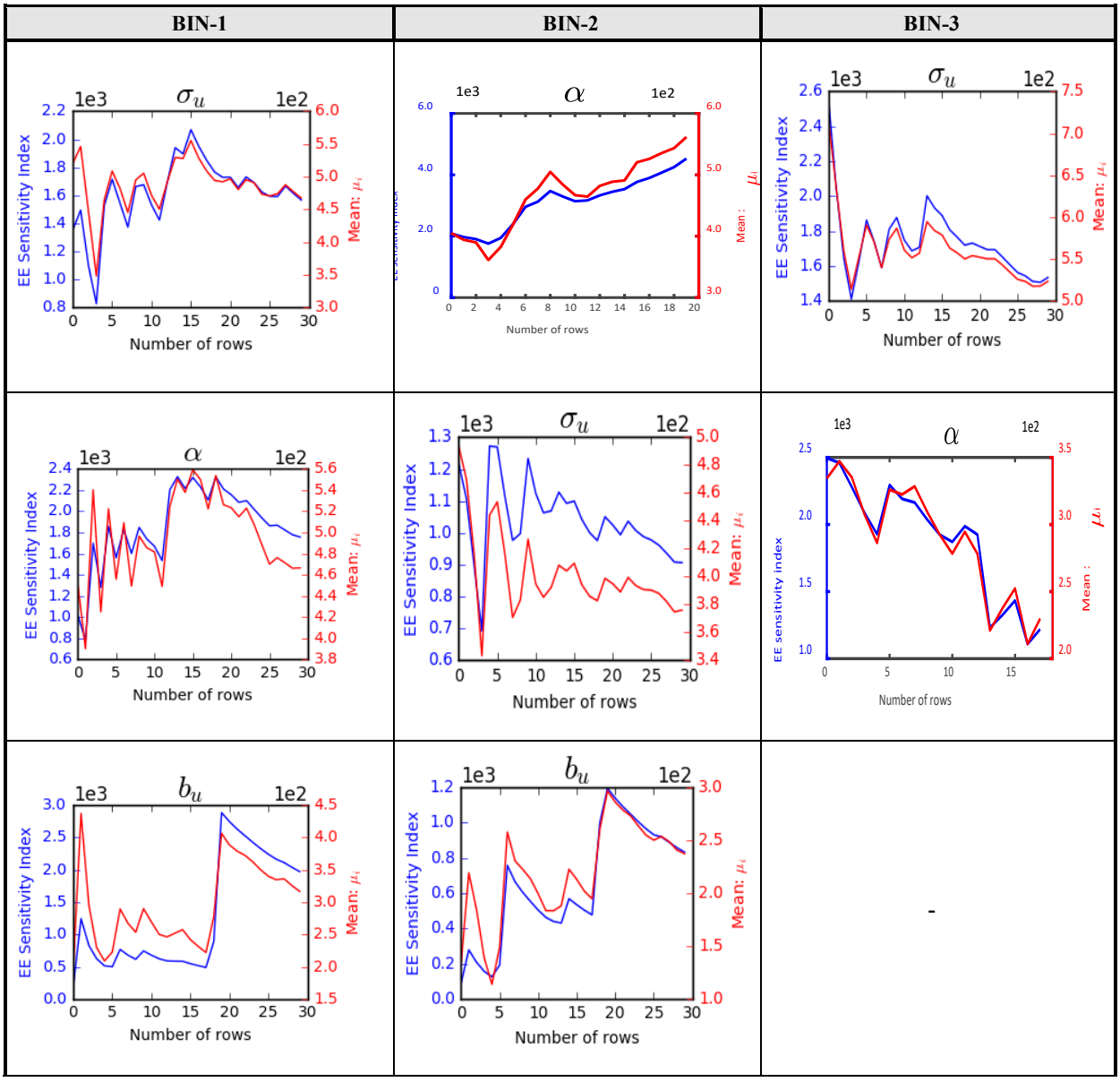

Figure 11. Elementary effects convergence for the top three sensitive parameter identified for rotor torque fatigue: mean (μ_i^*) and sensitivity index.

Acknowledgments

This work was supported by the U.S. Department of Energy under Contract No. DE-AC36-08GO28308 to the National Renewable Energy Laboratory. The U.S. Government retains and the publisher, by accepting the article for publication, acknowledges that the U.S. Government retains a nonexclusive, paid up, irrevocable, worldwide license to publish or reproduce the published form of this work, or allow others to do so, for U.S. Government purposes.

References

[1]IEC, "IEC 61400–1 Ed. 3. Wind Turbines – Part 1: Design Requirements," 2005.

[2] Holtslag, M., Bierbooms, W., and Bussel, G., "Wind Turbine Fatigue Loads as a Function of Atmospheric Conditions," *Wind Energy,* Vol. 19, 2016, pp. 1917–1932.

[3]Sathe, A., Mann, J., Barla, T., Bierbooms, A., and van Bussel, G., "Influence of atmospheric stability on wind turbine loads," *Wind Energy*, 2012.

[4]Sutherland, H., "Analysis of the Structural and Inflow Data from the LIST Turbine," Sandia National Laboratories Report, SAND2002-1838J, 2002.

[5]Eggers, A., Digumarthi, R., and Chaney, K., "Wind Shear and Turbulence Effects on Rotor Fatigue and Loads Control," *Transactions of the ASME*, Vol. 125, Nov. 2003.

[6]Nelson, L.D., Manuel, L., Sutherland, H.J., and Veers, P.S., "Statistical Analysis of Wind Turbine Inflow and Structural Response Data from the LIST Program," *Journal of Solar Energy Engineering,* Vol. 125, pp. 541–550.

[7]Saraynsoontorn, K., and Manuel, L., "On the Propagation of Uncertainty in Inflow Turbulence to Wind Turbine Loads," *Journal of Wind Engineering and Industrial Aerodynamics,* Vol. 96, 2008, pp. 508–523.

[8]Dimitrov, N., Natarajan, A., and Kelly, M., "Model of Wind Shear Conditional on Turbulence and Its Impact on Wind Turbine Loads," *Wind Energy*, Vol. 18, 2015, pp. 1917–1931.

[9]Wagner, R., Courtney, M., and Larsen, T., "Simulation of Shear and Turbulence Impact on Wind Turbine Performance," *Riso-R-Report 1722*, Jan. 2010.

[10]Ernst, B., and Seume, J., "Investigation of Site-Specific Wind Field Parameters and Their Effect on Loads of Offshore Wind Turbines," *Energies*, Vol. 5, 2012, pp. 3835–3855.

[11]Moriarty, P., Holley, W., and Butterfield, S., "Effect of Turbulence Variation on Extreme Loads Prediction of Wind Turbines," *Journal of Solar Energy Engineering*, Vol. 124, 2002, pp. 387–395.

[12]Solari, G., and Piccardo, G., "Probabilistic 3-D Turbulence Modeling for Gust Buffeting of Structures," *Probabilistic Engineering Mechanics*, Vol. 16, 2001, pp. 73–86.

[13]Walter, K., Weiss, C., Swift, A., Chapman, J., and Kelley, N., "Speed and Direction Shear in the Stable Nocturnal Boundary Layer," *Journal of Solar Energy Engineering*, Vol. 131, 2009.

[14]Burton, T., Jenkins, N., Sharpe, D., and Bossanyi, E., *Wind Energy Handbook*, 2011.

[15]Saltelli, A., et al., *Global Sensitivity Analysis, The Primer*, 2008.

[16]Kelly, M., Larsen, G., Dimitrov, N., and Natarjan, A., "Probabilistic Meteorlogical Characterization for Turbine Loads," *The Science of Making Torque from Wind*, Vol. 524, 2014.

[17]Bulaevskaya, V., Wharton, S., Cliftons, A., Qualley, G., and Miller, W., "Wind Power Curve Modeling in Complex Terrain Using Statistical Models," *Journal of Renewable and Sustainable Energy*, vol. 7, 2015.

[18]Kalverla, P., Steeeveld, G., Ronda, R., and Holtslag, A., "An Observational Climatology of Anamolous Wind Events at Offshore Meteomast Ijmuiden (North Sea)," *Journal of Wind Engineering and Industrial Aerodynamics*, Vol. 165, 2017, pp. 86–99.

[19]Park, J., Manuel, L., and Basu, S., "Toward Isolation of Salient Features in Stable Boundary Layer Wind Fields that Influence Loads on Wind Turbines," *Energies*, Vol. 8, 2015.

[20]Jonkman, B., "TurbSim User's Guide v2.00.00"

[21]Kelley, N., "Turbulence-Turbine Interaction: The Bases for the Development of the TurbSim Stochastic Simulator," NREL Report TP-5000-52353, 2011.

[22]Clifton, A., "135-m Meteorological Towers at the NWTC: Instrumentation, Data Acquisition and Processing," *Draft, https://wind.nrel.gov/MetData/Publications/.*

[23]Teunissen, H., "Characteristics of the Mean Wind and Turbulence in the Planetary Boundary Layer," *UTIAS 32*, Institute for Aerospace Studies, University of Toronto, 1970.

[24]Solari,G., "Turbulence Modelling for Gust Loading," *ASCE Journal of Structural Engineering*, Vol. 113, no.7, 1987, pp. 1550–1569.

[25]Saranyasontoorn, K., Manuel, L., and Veers, P.S., "A Comparison of Standard Coherence Models for Inflow Turbulence with Estimates from Field Measurements," *Journal of Solar Energy Engineering*, Vol. 126, November 2004.

[26]Moroz, E., "Time to Upgrade the Wind Turbine Suitability Process," *Presentation at AWEA WindPower 2017*.

[27]Lindelöw-Marsden,P., "Uncertainties in Wind Assessment with LIDAR," *Risø-R-1681UpWind Deliverable D1*, Risø National Laboratory for Sustainable EnergyTechnical University of Denmark, January 2009.

[28]Wharton, S., Newman, J.F., Qualley, G., and Miller, W.O., "Measuring Turbine Inflow with Vertically-Profiling Lidar in Complex Terrain," *J. Wind Eng. Ind. Aerodyn.,* Vol. 142, 2015, pp. 217–231.

[29]Berg, J., Mann, J., and Patten, E.G., "Lidar-Observed Stress Vectors and Veer in the Atmospheric Boundary Layer," *Journal of Atmospheric and Oceanic Technology*, Vol. 30, September 2013.

[30]Ziegler, L., and Muskulus, M., "Fatigue Reassessment for Lifetime Extension of Offshore Wind Monopile Substructures," *The Science of Making Torque from Wind*, Vol. 753, 2016.

[31]Saint-Geours, N., and Lilburne, L., "Comparison of Three Spatial Sensitivity Analysis Techniques," *Accuracy 2010 Symposium*.

[32]Dimitrov, N., and Berg, J., "2016 CCA: Wind2loads," *Presentation at Wind2loads Industry Webinar*, February 22nd, 2017.

[33]Matthuas, D., Bortolotti, P., Loganathan, J., and Bottasso, C., "A Study of the Propagation of Aero and Wind Uncertainties and their Effect on the Dynamic Loads of a Wind Turbine," *AIAA SciTech Forum*, 2017.

[34]Rinker, J., "Calculating the Sensitivity of Wind Turbine Loads to Wind Inputs Using Response Surfaces," *The Science of Making Torque from Wind*, Vol. 753, 2016.

[35]Crestaux, T., Maitre, O., Martinez, J., "Polynomial Chaos Expansion for Sensitivity Analysis," *Reliability Engineering and System Safety*, Vol. 94, 2009, pp. 1161–1172.

[36]Downey, R., "Uncertainty in Wind Turbine Life Equivalent Load due to Variation of Site Conditions," *M.Sc. Thesis Project* for the Technical University of Denmark, 2006.

[37]Martin, R., Lazakis, I., Barbouci, S., and Johanning, L., "Sensitivity Analysis of Offshore Wind Farm Operation and Maintenance Cost and Availability," *Renewable Energy*, Vol. 85, 2016, pp. 1226–1236.

[38]Francos, A., Elorza, F., Bouraoui, F., Bidoglio, G., and Galbiati, L., "Sensitivity Analysis of Distributed Environmental Simulation Models: Understanding the Model Behavior in Hydrological Studies at the Catchment Scale," *Reliability Engineering and System Safety*, Vol. 79, 2003, pp. 205–218.

[39]Sohier, H., Piet-Lahanier, H., and Farges, J., "Analysis and Optimization of an Air-Launch-to-Orbit Separation," *Acta Astronautica*, Vol. 108, 2015, pp. 18–29.

[40]Sumner, T., Shephard, E., and Bogle, I., "A Methodology for Global-Sensitivity Analysis of Time-Dependent Outputs in Systems Biology Modelling," *Journal of the Royal Society Interface*, Vol. 9, 2012, pp. 2156–2166.

[41]Huang, Y., and Pierson, D., "Identifying Parameter Sensitivity in Water Quality Model of a Reservoir," *Water Quality Research Journal of Canada*, Vol. 47, 2012, pp. 451–462.

[42]Gan, Y. et al., "A Comprehensive Evaluation of Various Sensitivity Analysis Methods: A Case Study with a Hydrological Model," *Environmental Modelling and Software*, Vol. 51, 2014, pp. 269–285.

[43]Saranyasoontorn, K., and Manuel, L., "On the Study of Uncertainty in Inflow Turbulence Model Parameters in Wind Turbine Applications," *44th AIAA Aerospace Sciences Meeting and Exhibit*, 9–12 January 2006, Reno, Nevada.

[44]Campolongo, F., Cariboni, J., and Saltelli, A., "An Effective Screening Design for Sensitivity Analysis of Large Models," *Environmental Modelling and Software* Vol. 22, 2007, pp. 1509–1518.

[45]Campolongo, F., Saltelli, A., and Cariboni, J., "From Screening to Quantitative Sensitivity Analysis. A Unified Approach," *Computer Physics Computations*, Vol. 182, 2011, pp. 978–988.

[46]Jansen, M., "Analysis of Variance Designs for Model Output," *Computer Physics Communication*, Vol. 117, 1999, pp. 35–43.

[47]Jonkman, J., Butterfield, S., Musial, W., and Scott, G., "Definition of a 5-MW Reference Wind Turbine for Offshore System Development," *NREL/TP-500-38060*, Golden, CO: National Renewable Energy Laboratory, February 2009.